Journal of the Brazilian Society of Mechanical Sciences and Engineering manuscript No.
(will be inserted by the editor)

A well simulator for homogeneous reservoirs based on formulations of the isogeometric boundary element method

Lúcio G. Nascimento · Gustavo S. V. Gontijo · Éder L. Albuquerque · Lucas S. Campos · Jon Trevelyan · Eugênio L. F. Fortaleza

Received: date / Accepted: date

Abstract The development of a simulator for homogeneous reservoirs with application in producer wells (represented by a sink) and the aquifer analysis is obtained by combining the Boundary Element Method (BEM), the Isogeometric Formulation using NURBS (Non Uniform Rational B-Spline) as shape functions, and also the Axisymmetric Formulation.

The Isogeometric Formulation makes the discretization of geometric model (mesh generation), which is the step of numerical analysis that is more time consuming for the engineer, be no longer necessary, since the same functions that describe the geometry also approximate the field variables in the BEM. In other words, the same discretization used in the geometric model, generated in CAD (Computer Aided Design) modeling programs, also is used by the BEM.

The oil and water reservoirs, as simplified models for validation of the new mathematical methodology, can be fully represented by the analysis of a plane passing through the axis of rotational (axial) symmetry. The dimension of the problem is reduced from three to two dimensions: radial and axial directions only, and all variables in the circumferential direction are assumed to be constant. When the geometry and the problem variables are both axisymmetric, then the problem is considered fully axisymmetric.

The isogeometric and axisymmetric formulations are coupled to obtain the well simulator for the single and double phase case, i.e. one or two incompressible fluids inside the reservoir. The determination of boundary conditions for the model, including the analysis of fluids interface movement, is also presented. The final code is a new tool for the analysis of gas/water coning phenomenon and quick drawdown problem in homogeneous reservoirs, as validation models. Validation of the results is carried out by comparing with others numerical methods and analytical results.

Keywords Gas coning · Water coning · Porous media · Boundary element method · Isogeometric formulation · Axisymmetric formulation · Well simulator · Aquifer analysis

The Authors would like to acknowledge the Brazilian institutions: CNPq, CAPES, FINEP and MCT for supporting the present study.

Lúcio G. Nascimento
ORCID: 0000-0002-6464-7255

Éder L. Albuquerque
ORCID: 0000-0002-7154-6946

Lucas S. Campos
Federal University of Espirito Santo, Department of Mechanical Engineering, 29075-910, Vitoria, ES, Brazil.

Jon Trevelyan
Durham University, DH1, Durham, United Kingdom.

All authors
University of Brasilia, Department of Mechanical Engineering, 70910-900, Brasilia, DF, Brazil.

1 Introduction

The cost of implanting an oil production plant (onshore or offshore) is quite high, even by the standards of a consolidated member company of this market. High productivity is always desired, regardless of the prospecting conditions. This means producing the largest quantity of a ”clean” oil and gas with lower concentration of methane. Only for optimum conditions, however, it is possible to obtain extraction at the desired speed and purity. There are several factors that limit production in a real case scenario, from the extraction through the well in the reservoir characterized by the multiphase flow in porous media, as the multiphase flow in the transport line, the pipeline-riser system, as well as insurgent problems in separators, manifold and others.

The present work proposes a well simulator in order to study formations of the gas and water coning, conditions detrimental to the production since there is infiltration of other fluids with greater mobility than petroleum, flowing toward the well in form of a cone, according to the potential gradient. The same simulator is also applied in aquifer (water reservoir) analysis to study a quick drawdown problem. It is constructed using the Isogeometric Boundary Element Method (IGA-BEM), which has numerical advantages not only with respect to other numerical methods such as the Finite Difference Method (FDM), Finite Volume Method (FVM), Finite Element Method (FEM), but also to the conventional Boundary Element Method (BEM). The IGA-BEM uses NURBS (Non Uniform Rational B-Spline) geometries that brings greater smoothness to the curves of the elements in question and ensure the continuity of the variables of field, derived and geometry.

The phenomena of the gas or water coning are limiting factors in the productivity of an oil well, as they occur due to the pressure gradient applied by the well in order to extract the oil from the reservoir. Figure 1 shows an example of oil reservoir coexisting water and gas coning. The pressure gradient reaches all the fluids present in the reservoir (oil, water, natural gas). As water and gas have greater mobility than oil, they tend to flow towards the well, taking the form of a cone. For certain extraction flow values, the water coning and/or gas coning reach the end of well causing water and/or gas production along with oil, thereby reducing productivity.

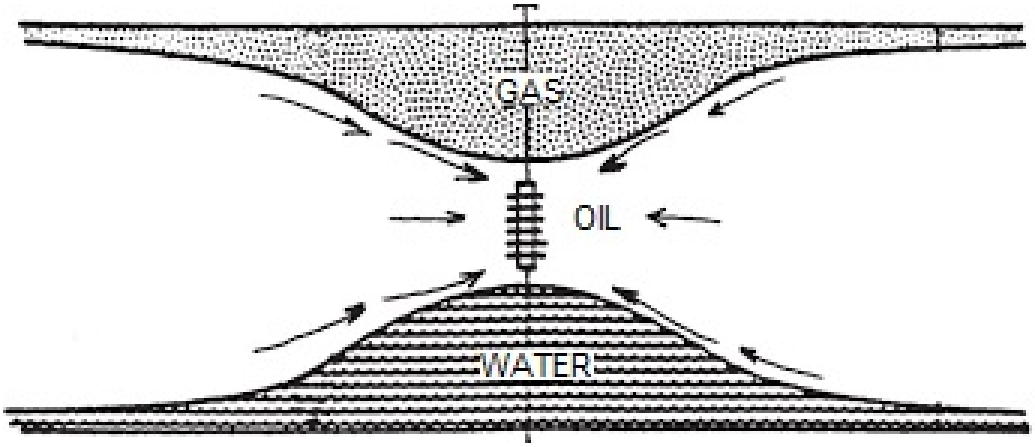

Fig. 1: Oil reservoir coexisting water and gas coning

Analytical treatments with severe approximations and restrictions were used in the formulation of several models and correlations that are used to estimate the behavior of water and gas coning in order to overcome the great complexity of the problem (Dake [1], Fortaleza et al. [2]). Nowadays there are advanced numerical analysis tools that allow the study of these phenomena through computer simulation, e.g., OPM (Open Porous Media), BOAST, MRST (Matlab Reservoir Simulation Tool), Reveal, tNavigator, IX, Eclipse, etc.; minimizing the simplifications in models used and increasing the accuracy of results obtained. In this work, the new tool developed is applied for gas and water coning simulator in homogeneous reservoirs and quick drawdown in aquifers, as a proposal for simple models, to validate the Isogeometric Boundary Element Method with

application in axisymmetric problems. Axisymmetric geometries are formed by rotating 360° from a two-dimensional plane on a given axis, known as the rotational symmetry axis. The z axis is the rotational or axial symmetry axis, while r and θ are the radial and circumferential directions, respectively, used in the cylindrical coordinates. The oil or water reservoir, as simplified models for validation of the new mathematical methodology, can be considered as an axisymmetric geometry.

The main aim of this work leads to the implementation of a new mathematical methodology through the Isogeometric Formulation in conjunction with the Axisymmetric Formulation, to achieve the fundamental solutions of the simplified problem and present as a model for validation - the phenomenons of the gas and water coning in homogeneous reservoirs and quick drawdown problem in aquifers. The efficiency of the code compiling, from this new mathematical tool, is still being implemented through an ACA (Adaptive Cross Approximation) accelerator. Therefore, it is not the scope of this work to deal with simulation efficiency, but rather to present the functioning of the new mathematical methodology within BEM.

A possibility to expand the formulation for heterogeneous media, that is been analyzed, it is the use of multiple domains as suggested by Ramsak and Skerget [3].The basic idea of the multi domain method is to write the integral equations for each sub domain individually and then couple the sub domains under interface boundary conditions. The resulting system matrix will be sparse and block-banded, similar to the FEM. In this manner, heterogeneous media can be easily modeled. Apart from this, the memory and CPU demands could be reduced significantly as shown by Ramsak and Skerget [3].

2 Theoretical model

In this work, the formulation of Isogeometric Boundary Element Method with axisymmetric fundamental solutions is presented for problems governed by the Laplace equation; model adopted to the analysis of potential flow. The fundamental solution applied corresponds to the potential response in an infinite medium when the sink (or source) is concentrated at a point on the domain.

In order to obtain the oil extraction formulation and aquifer (water reservoir) analysis, it is used a simple yet powerful tool is used in the qualitative evaluation of the factors affecting multiphase flow in porous media, Darcy's Law. For two-dimensional or three-dimensional flow, one has:

$$\mathbf{q} = -K\nabla\Phi \tag{1}$$

where Φ is the fluid column height and K is the hydraulic conductivity of the medium, defined by Bear [4] as:

$$K = \frac{\kappa\rho g}{\mu} \tag{2}$$

From Eq. (2), κ is the absolute permeability of the porous media, ρ is the specific mass of the fluid, μ is the dynamic viscosity of the fluid and g is the gravity acceleration. The permeability κ is a characteristic of the porous media and it is independent of the fluid that is filling it. The hydraulic conductivity K involves the specific mass and the dynamic viscosity of the fluid, ρ and μ, respectively, and therefore it is dependent on the fluid that is flowing.

The limiting factors of Darcy's Law lie in the permeability of porous media that can undergo considerable changes as a function of the void volume of material and the fluid temperature at the time of testing. The same soil may have, according to its situation, a different permeability.

By Eq. (1), it can be seen that the apparent velocity vector of the fluid, $\mathbf{q}$, is linearly related (through the hydraulic conductivity of the medium) to the gradient of a potential function. This function is called the flow velocity potential. Liggett and Liu [5] define it through the piezometric height, given by the following expression:

$$\Phi = \frac{p}{\rho g} + z \tag{3}$$

The first term of Eq. (3) is therefore known as piezometric height; the second term being the height that is associated with a referential or, still, as the energy associated with the position of fluid in the gravitational field.

Liggett and Liu [5] further define the real average velocity vector of the fluid inside pores $\mathbf{u}$ as:

$$\mathbf{u} = \frac{\mathbf{q}}{n} \tag{4}$$

where n is the porosity of medium.

The fluids, as well as the medium, are considered incompressible in the adopted potential flow model. The porous media is homogeneous with constant permeability and isotropic in the region of flow, and also, the dynamic viscosity of the fluids is considered to be constant. In this model, the pores are saturated with only one fluid at a time.

From the Eq. (1) and the incompressible continuity equation, considering yet the flow to be irrotational, it has:

$$\nabla \cdot (-K \nabla \Phi) = 0 \tag{5}$$

Considering the medium as being homogeneous, the hydraulic conductivity K is assumed to be constant. Therefore, Eq. (5) becomes:

$$\nabla^2 \Phi = 0 \tag{6}$$

Equation (6) is defined as the Laplace Equation, which governs the flow in a porous media. In the present work, a point sink must be added to be counted in the hydrodynamics of the oil reservoir problem. Thus, applying the principle of mass conservation, it is obtained:

$$\nabla \cdot \mathbf{q} = -Q\,\delta(\mathbf{x} - \mathbf{x_s}) \tag{7}$$

Rearranging Eq. (7) from Eq. (1), it becomes:

$$\nabla^2 \Phi = \frac{Q}{K}\,\delta(\mathbf{x} - \mathbf{x_s}) \tag{8}$$

where δ is the Dirac delta function and $\mathbf{x_s}$ is the position vector of the sink.

Equation (8) defines the laplacian of potential function to be equal 0 in the entire domain, thus becoming the Laplace equation. At the point where sink is located, the Laplace equation becomes the Poisson equation.

Compressible flow is not considered in this work. Therefore, the governing equation of compressible flow in porous media, i.e, the hydraulic diffusivity equation, is not analyzed. In flow regions where the irrotational approach is adequate, the solution to the problem is valid for any incompressible fluid, where its specific mass or viscosity has no influence. Time does not appear in the incompressible continuity equation, thus, the solution is valid even instantaneously for non-permanent flow. To satisfy the Laplace equation and boundary conditions existing at that moment, the incompressible flow field is adjusted instantly. This approach can be applied to the interface movement problem studied in this work, where the Laplace equation is calculated step by step at each time instant.

The solutions obtained for irrotational flows are therefore approximations to complete solutions of the Navier-Stokes equation. When this approach is not adequate is needed to solve the Navier-Stokes through numerical methods as the CFD (Computational Fluid Dynamics).

2.1 Isogeometric formulation

The Isogeometric Analysis is an attempt to eliminate the generation of mesh using the discretization of Computer Aided Design (CAD) software, where the BEM has significant advantages. The predominant technology used by CAD in the representation of complex geometries is the Non-Uniform Rational B-Spline (Lin [6]). This makes possible to accurately reproduce entities that would only be approximated by polynomial functions, including circular conic sections, cylinders, spheres, ellipsoids, paraboloids, etc. There is a vast literature dealing with the different aspects of NURBS (e.g. Piegl and Tiller [7], Rogers [8], Farin [9], Piegl [10], Lamousin [11], Hughes, Reali and Sangalli [12], Temizer, Wriggers and Hughes [13]). NURBS have been used successfully in fluid mechanics problems by Nielsen [14] et al., Bazilevs [15] et al., Bazilevs and Akkerman [16]. The years of research have resulted in several efficient algorithms for fast assessment and refinement.

The main concept presented in Hughes, Cottrell and Bazilevs [17] is to use NURBS not only as a discretization of geometry, but also as a discretization tool in the analysis, assigning the denomination of isogeometric analysis to this characteristic of methods. In the BEM, a formulation using B-Splines is presented initially in Cabral et al. [18] and Cabral, Wrobel and Brebbia [19], but still without concern for integration into CAD. This integration was later observed in Simpson et al. [20] and Simpson et al. [21]. The Isogeometric concept is also present in mesh-free methods, creating spline-based methods, as presented in Wang and Zhang [22], Shaw and Roy [23], Kim and Youn [24].

Campos et al. [25] presents an Adaptive Cross Approximation (ACA) accelerated Isogeometric Boundary Element Method (IGA-BEM) using Non-Uniform Rational B-Splines (NURBS) as shape and interpolation functions. The developed formulations are implemented and applied in the analysis of several numerical examples and their results are compared with the Boundary Element Method with the use of polynomial shape functions. Unlike conventional BEM, the boundary conditions in the isogeometric formulation can not be applied directly to the problem, since the control points are typically outside the boundary. To overcome this problem, it uses a transformation matrix **E** for B-Splines that can relate the values between the control points and the collocation points.

NURBS can represent exact conic sections: circles, hyperboles, ellipses, and parables. Since the usual Lagrangian shape functions are not able to describe more complex geometries in a exact way, NURBS are better suited to represent the geometries and can also be used to approximate the field variables. The main application of the NURBS functions in this work is presenting a new analysis of the gas/water coning at the interface for critical flows. In future works, high heterogeneous media could be modeled with the implementation of multiple domains as a more complex case of application.

The NURBS can be calculated by the following expression:

$$C(t) = \frac{\sum_{i=1}^{n+1} B_i N_{i,k}(t)\,\omega_i}{\sum_{i=1}^{n+1} N_{i,k}(t)\,\omega_i} = \sum_{i=1}^{n+1} B_i R_{i,k}(t) \tag{9}$$

where t is the curve parameter and $R_{i,k}(t)$ is the rational basis function given by:

$$R_{i,k}(t) = \frac{N_{i,k}(t)\,\omega_i}{\sum_{i=1}^{n+1} N_{i,k}(t)\,\omega_i} \tag{10}$$

$\sum_{i=1}^{n+1} B_i N_{i,k}(t)$ is the B-Spline curve, where B_i are the control points, $N_{i,k}(t)$ are the basis functions of order k and degree $k-1$, and ω_i is the weight function associated with the specific control point i. The basis function is defined as:

$$N_{i,k}(t) = \frac{(t-u_i)}{u_{i+k-1}-u_i} N_{i,k-1}(t) + \frac{(u_{i+k}-t)}{u_{i+k}-u_{i+1}} N_{i+1,k-1}(t) \tag{11}$$

where u_i are the values of **U** knots vector, defined by a series of increasing real parameters and has a strong influence on the basis functions of a B-Spline.

B-Splines are a generalized form of the Bezier curves. Therefore, NURBS is a generalization of B-Spline, replacing the polynomial base with a polynomial ratio.

2.2 Axisymmetric formulation

In axisymmetric problems, the dimension of problem is reduced from three to two dimensions: radial and axial directions only, and all variables in the circumferential direction are assumed as constant. A large number of engineering applications (structures or components) are axisymmetric or can be approximated as axisymmetric, for example pressure vessels, mechanical seals, pipelines and even an oil or water reservoir. Lucas [26] studied the phenomenon of water coning in an oil reservoir through the solutions of Axisymmetric Boundary Integral Equation. Some axisymmetric geometries may be under nonaxisymmetric loading, such as wind forces on a cooling tower. In these cases special treatment is required to solve the problem.

Unlike other numerical methods (such as the Finite Element Method), the Boundary Element Method for axisymmetric problems is not a simple transformation of the two-dimensional formulation. It requires a greater mathematical effort when compared to two and three-dimensional formulations. There are basically two types of approximations for axisymmetric formulations: (I) derive from axisymmetric fundamental solutions based on circular loads as opposed to loads point; (II) from the integral in relation to the circumferential direction of the three-dimensional solutions. Both approaches lead to identical solutions and have been discussed in detail for potential, elastic, thermoelastic, and centrifugal problems since Bakr [27] and Becker [28]. In this work only the second approximation is detailed, that is, from the three-dimensional solutions.

There are three directions of cylindrical or curvilinear coordinates: radial (r), axial (z) and circumferential (θ). To reduce the system by one dimension, the three-dimensional solution is then transformed from the Cartesian coordinates (x,y,z) into cylindrical coordinates (r,θ,z) and then integrates analytically with respect to the circumferential direction, θ , in order to produce cores and functions with radial and axial components only.

The Laplace equation, Eq. (6), can be written in cylindrical coordinates for three-dimensional domain as follows:

$$\nabla^2\Phi_{3D} = \frac{\partial^2\Phi}{\partial r^2} + \frac{1}{r}\frac{\partial\Phi}{\partial r} + \frac{1}{r^2}\frac{\partial^2\Phi}{\partial\theta^2} + \frac{\partial^2\Phi}{\partial z^2} = 0 \tag{12}$$

and polar coordinates, for two-dimensional domain, as:

$$\nabla^2\Phi_{2D} = \frac{1}{r}\frac{\partial}{\partial r}\left(r\frac{\partial\Phi}{\partial r}\right) + \frac{1}{r^2}\frac{\partial^2\Phi}{\partial\theta^2} = 0 \tag{13}$$

All variables are constant with respect to the circumferential direction for axisymmetric problems, thus all derivatives with respect to θ are equal zero. Thus Eq. (12) and Eq. (13), respectively, becomes:

$$\nabla^2\Phi_{axi} = \frac{\partial^2\Phi}{\partial r^2} + \frac{1}{r}\frac{\partial\Phi}{\partial r} + \frac{\partial^2\Phi}{\partial z^2} = 0 \tag{14}$$

$$\nabla^2\Phi_{2D} = \frac{1}{r}\frac{\partial}{\partial r}\left(r\frac{\partial\Phi}{\partial r}\right) = 0 \tag{15}$$

where $3D$, $2D$ and axi are the subscripts referring to the three-dimensional, two-dimensional and axisymmetric solutions, respectively.

The axisymmetric fundamental solution for the velocity potential Φ^*_{axi} is based on an arc of potentials placed along the point p, as opposed to a potential point for the three-dimensional solution. Therefore, the expression for axisymmetric fundamental solution is given by:

$$\Phi^*_{axi} = \int_0^{2\pi}\Phi^*_{3D}d\theta_Q \tag{16}$$

The three-dimensional fundamental solution, Φ^*_{3D}, corresponding to the potential response in an infinite porous media is given by the following expression according Becker [28]:

$$\Phi^*_{3D} = \frac{1}{4\pi K}\frac{1}{r(p,Q)} \tag{17}$$

where $r(p,Q)$ is the corresponding distance between the load point p, and the field point Q, K is the hydraulic conductivity of the porous media.

After suitable mathematical steps, the axisymmetric fundamental solution to the velocity potential can be rewritten as:

$$\Phi^*_{axi} = \frac{1}{\pi KC} K_e(m, \pi/2) \tag{18}$$

where C and m are parameters related to the load point and field point coordinates and $K_e(m,\pi/2)$ is the elliptic integral of the first kind (Becker [28]).

From Eq. (18) is possible to obtain the axisymmetric fundamental solution of velocity through its derivative with respect to the normal direction multiplied by the hydraulic conductivity of the porous media, defined as:

$$q^*_{axi} = -K\frac{\partial \Phi^*_{axi}}{\partial \mathbf{n}} \tag{19}$$

The expression for two-dimensional fundamental solution of the velocity potential Φ^*_{2D} for same problem conditions, after a few more mathematical steps, is given according Katsikadelis [29]:

$$\Phi^*_{2D} = -\frac{1}{2\pi K} \ln r(p,Q) \tag{20}$$

Equation (20) is also applied for the Eq. (19) to obtain the two-dimensional fundamental solution of velocity. It becomes:

$$q^*_{2D} = -K\frac{\partial \Phi^*_{2D}}{\partial \mathbf{n}} = \frac{1}{2\pi r^2(p,Q)} \left[r_x(p,Q)\,\mathbf{n_x} + r_z(p,Q)\,\mathbf{n_z} \right] \tag{21}$$

where $r_x(p,Q)$ and $r_z(p,Q)$ are the components of distance between load point and field point; $\mathbf{n_x}$ and $\mathbf{n_z}$ are components of the normal vector.

3 Well Simulator

By applying the NURBS to shape functions, the BEM is now referred as Isogeometric Boundary Element Method. The sum of all the Isogeometric Boundary Elements will then be a representation that, in most cases, it will be the actual representation of the boundary, denoted by Γ.

Each part of the boundary is approximated by one or more Bezier curves with a continuity mechanism between the segments. Knowing that $R_{i,k}(t)$ is the rational basis function of order k (that influences a given region of a NURBS curve), the approximation with isogeometric boundary elements becomes:

$$c\Phi(x_d,y_d) = \int_\Gamma \sum_{i=1}^{n+1} \Phi^c_i R_{i,k}(t)\, q^*(x_d,y_d)\, d\Gamma - \int_\Gamma \sum_{i=1}^{n+1} q^c_i R_{i,k}(t)\, \Phi^*(x_d,y_d)\, d\Gamma \tag{22}$$

where Φ^c_i and q^c_i are the potential and velocity, respectively, at the control point i and the therm c is a multiplying constant.

Equation (22) takes two different forms: two-dimensional and axisymmetric domain. For the two-dimensional domain becomes:

$$c\Phi(x_d,y_d) = \sum_{i=1}^{n+1} \left(\Phi^c_i \int_\Gamma R_{i,k}(t)\, q^*_{2D}(x_d,y_d)\, d\Gamma \right) - \sum_{i=1}^{n+1} \left(q^c_i \int_\Gamma R_{i,k}(t)\, \Phi^*_{2D}(x_d,y_d)\, d\Gamma \right) \tag{23}$$

Equation. (23) is called discretized Isogeometric Boundary Integral Equation for two-dimensional domain. For axisymmetric problems, where the fundamental solutions for potential and velocity are axisymmetric, the discretized Isogeometric Boundary Integral Equation is given by:

$$c\Phi(x_d,y_d) = \sum_{i=1}^{n+1}\left(\Phi_i^c \int_\Gamma R_{i,k}(t)\, q^*_{axi}(x_d,y_d)\, x\, d\Gamma\right) - \sum_{i=1}^{n+1}\left(q_i^c \int_\Gamma R_{i,k}(t)\, \Phi^*_{axi}(x_d,y_d)\, x\, d\Gamma\right) \tag{24}$$

After the boundary is parameterized by t and the use of Gauss quadrature, Eq. (23) and Eq. (24) can be rearranged with the terms of $\mathbf{H}$ matrix on one side and the terms of $\mathbf{G}$ matrix on the other:

$$\sum_{i=1}^{n+1} H_{i,k}\Phi_i^c = \sum_{i=1}^{n+1} G_{i,k} q_i^c \tag{25}$$

or by the matrix form:

$$\mathbf{H}\Phi^c = \mathbf{G}\mathbf{q}^\mathbf{c} \tag{26}$$

The superscript c have influence on k elements of matrix $\mathbf{H}$, which does not occur in conventional BEM. Equation (26) is the discretized Boundary Integral Equation, represented in matrix form. In the case where governing equation has a point sink, that is, the governing equation is not Laplace's, but Poisson's, Eq. (26) becomes:

$$\mathbf{H}\Phi^c = \mathbf{G}\mathbf{q}^\mathbf{c} - \mathbf{s} \tag{27}$$

where $\mathbf{s}$ is the vector that holds the contribution of each point sink. Each element of this vector corresponds to the effect of sinks at a given source point d, represented by:

$$s_d = \sum_{j=1}^{n_s} Q_j \Phi^* \tag{28}$$

where n_s is the number of punctual sinks of the problem, Q_j is the intensity of sink, and Φ^* is the fundamental solution of the potential, ranging in magnitude for axisymmetric problems.

In order to separate the known variables from the unknown, it is necessary to reorganize the equation through a matrix system. Therefore, it can be written as:

$$\mathbf{A}\mathbf{x} = \mathbf{b} - \mathbf{s} \tag{29}$$

or

$$\mathbf{x} = \mathbf{A}^{-1}(\mathbf{b} - \mathbf{s}) \tag{30}$$

Through the linear system given by Eq. (30), it is possible to obtain the unknown values of the potential Φ and the velocity $\mathbf{q}$ on the control points. However, it should be noted that the control points are typically outside the boundary, i.e., the boundary conditions cannot be applied directly. A transformation matrix $\mathbf{E}$ for B-Splines is then used to overcome this problem (Cabral et al., [18]). This matrix uses the basis functions to relate the values at control points to the values at collocation points, through the following:

$$\Phi = \mathbf{E}\Phi^c \tag{31}$$

$$\mathbf{q} = \mathbf{E}\mathbf{q}^\mathbf{c} \tag{32}$$

where the vectors Φ and $\mathbf{q}$ contain the values for potential and velocity, respectively, at the collocation points; while Φ^c and $\mathbf{q}^\mathbf{c}$ contain the values for potential and velocity, respectively, at the control points. The same idea can be applied to NURBS.

Replacing the Eq. (31) and (32) in the Eq. (27), it has:

$$\mathbf{H}\mathbf{E}^{-1}\Phi = \mathbf{G}\mathbf{E}^{-1}\mathbf{q} - \mathbf{s} \tag{33}$$

Equation (33) can be solved in the usual manner as conventional BEM.

3.1 New positions of control points

Through the phenomena of gas/water coning in oil reservoir and aquifer analysis, a moving interface between the fluids is present in the problem. In order to quantify this movement, the method of control points repositioning (Piegl and Tiller, [10]) is used. The repositioning of control points takes place in a NURBS curve. From Eq. (9) for the NURBS curve, an arbitrary control point B_i will undergo a translation to $\hat{B}_i$ through a vector $\mathbf{V}$, given by:

$$\mathbf{V} = \hat{B}_i - B_i \tag{34}$$

Therefore, the new curve for the transferred arbitrary control point becomes:

$$\begin{aligned} \hat{C}(t) &= B_1 R_{1,k}(t) + \ldots + (B_i + \mathbf{V}) R_{i,k}(t) + \ldots + B_{n+1} R_{n+1,k}(t) \\ &= C(t) + R_{i,k}(t)\,\mathbf{V} \end{aligned} \tag{35}$$

Equation (35) expresses the functional translation of all points of the curve $C(t)$ in which t (curve parameter) $\in [t_i, t_{i+k})$. All points on the curve outside this range are not affected. Applying Eq. (35) to $n+1$ control points, it is possible, therefore, to compute the total interface movement.

Considering that collocation points move only in z direction; there is a function F, defined by the interface as a material line. The velocity at interface is the velocity of material points that defines it. As a function of this calculated velocity, it is possible to deduce the equation that defines its position:

$$F = z - \lambda(x,t) = 0 \tag{36}$$

where $\lambda(x,t)$ is the function that expresses the height of interface for a given coordinate x and a certain time t.

Differentiating Eq. (36), it has:

$$\frac{DF}{Dt} = \frac{\partial F}{\partial t} + \frac{\mathbf{q}}{n} \cdot \nabla F = 0 \tag{37}$$

where $\frac{\mathbf{q}}{n}$ is the real average velocity vector of the fluid inside pores given by Eq. (4).

Replacing the Eq. (36) in the Eq. (37), it has:

$$\frac{DF}{Dt} = -\frac{\partial \lambda}{\partial t} + \frac{\mathbf{q}}{n} \cdot (\nabla z - \nabla \lambda) = 0 \tag{38}$$

which can be written as

$$\frac{\partial \lambda}{\partial t} = \frac{1}{n} (\mathbf{q} \cdot \hat{\mathbf{e}}_\mathbf{z} - \mathbf{q} \cdot \nabla \lambda) \tag{39}$$

Applying the Eq. (1), it is obtained:

$$\frac{\partial \lambda}{\partial t} = -\frac{K}{n} \left(\frac{\partial \Phi}{\partial z} - \nabla \Phi \cdot \nabla \lambda \right) \tag{40}$$

A relation between $\frac{\partial \lambda}{\partial t}$ and $\frac{\partial \Phi}{\partial \mathbf{n}}$ is sought:

$$\frac{\partial \Phi}{\partial \mathbf{n}} = \nabla \Phi \cdot \hat{\mathbf{e}}_\mathbf{n} \tag{41}$$

where the unit normal vector may be written as:

$$\hat{\mathbf{e}}_\mathbf{n} = \frac{\nabla (z - \lambda)}{|\nabla (z - \lambda)|} \tag{42}$$

Replacing Eq. (42) at Eq. (41), it has:

$$\frac{\partial \Phi}{\partial \mathbf{n}} = \frac{\frac{\partial \Phi}{\partial z} - \nabla \Phi \cdot \nabla \lambda}{|\nabla (z - \lambda)|} \tag{43}$$

where

$$\frac{\partial \Phi}{\partial z} = \frac{\partial \Phi}{\partial \mathbf{n}} |\nabla (z - \lambda)| + \nabla \Phi \cdot \nabla \lambda \tag{44}$$

Replacing Eq. (44) at Eq. (40), it comes:

$$\frac{\partial \lambda}{\partial t} = -\frac{K}{n} \frac{\partial \Phi}{\partial \mathbf{n}} |\nabla (z - \lambda)| \tag{45}$$

The quantity $|\nabla (z - \lambda)|$ in Eq. (45) can be written as:

$$|\nabla (z - \lambda)| = \left[1 + \left(\frac{\partial \lambda}{\partial x} \right)^2 \right]^{1/2} \tag{46}$$

and

$$\cos \eta = \left[1 + \left(\frac{\partial \lambda}{\partial x} \right)^2 \right]^{-1/2} \tag{47}$$

where $\tan \eta$ is defined as the free surface slope: $\partial \lambda / \partial x = -\tan \eta$.

Replacing Eq. (47) and Eq. (46) at Eq. (45), it arrives:

$$\frac{\partial \lambda}{\partial t} = -\frac{K}{n} \frac{\partial \Phi}{\partial \mathbf{n}} \left[1 + \left(\frac{\partial \lambda}{\partial x} \right)^2 \right]^{1/2} = -K \frac{\partial \Phi}{\partial \mathbf{n}} \frac{1}{n \cos \eta} \tag{48}$$

The information obtained is the normal velocity vector $\mathbf{q}$ to the collocation point. Thus, the Eq. (48) in terms of this normal velocity vector projected on the z axis is:

$$\frac{\partial \lambda}{\partial t} = \frac{1}{n} \frac{\mathbf{q}}{\cos \eta} \tag{49}$$

where η is the angle formed between the normal velocity vector to the collocation point and the z-axis.

Equation (49) is the equation for simulation of free surface movement. The implementation of this equation must be made in such a way as to take into account the size of time step used in the iterations. Writing Eq. (49) in terms of finite differences (Zhang et al., [30]), it has:

$$z_{m+1} = z_m - \frac{\Delta t}{n \cos \eta} \left[\beta \left(\mathbf{q} \cdot \hat{e}_z \right)_{m+1} + (1 - \beta) \left(\mathbf{q} \cdot \hat{e}_z \right)_m \right] \tag{50}$$

where β is a weighting factor; z is the height of interface; Δt is the size of time step and the sub-indices m and $m+1$ are, respectively, the current and next immediate time step.

The interface is considered abrupt where capillary stresses are admitted to be negligible.

3.2 Boundary conditions

As already described, the governing equation of potential flow is the Laplace Equation - Eq. (6), written in terms of the potential Φ. The boundary conditions applicable to each knot are of known potential or known velocity. The reservoir has two configurations: single phase, i.e. only one incompressible fluid inside the reservoir; double phase, i.e. two incompressible fluids inside the reservoir.

3.2.1 Potential Single Phase Flow

The well simulator for single phase flow (only one incompressible fluid inside the reservoir) is used to simulate an oil extraction subject to the occurrence of a gas coning, that is, for the reservoir configuration where one layer of oil and another layer of gas coexist. Figure 2 shows the general appearance of an oil reservoir problem.

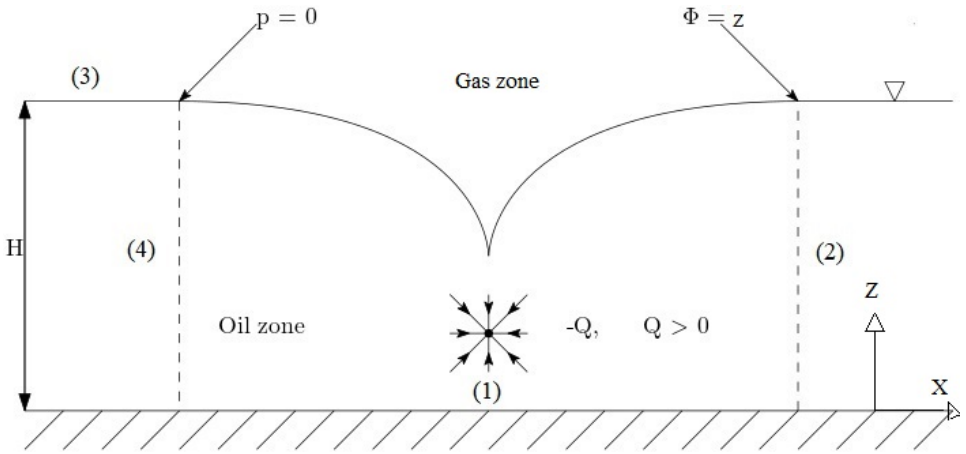

Fig. 2: Gas Coning Phenomenon - Boundary Conditions: (1) impermeable boundary ($q = 0$); (2) and (4) known potential boundary; (3) interface boundary

The parameters used in the code are set out in Table 1 below.

Table 1: Parameters used in the code

Quantities	Nomenclature	Measurement unit (SI)
Specific mass	ρ	kg/m^3
Dynamic viscosity	μ	Pa.s
Medium porosity	n	–
Absolute permeability	κ	m^2
Hydraulic conductivity	K	m/s
Potential	Φ	m
Well intensity	Q	m^2/s
Well coordinates	(x_p, z_p)	m
Total time	t_t	s
Running pump time	t_p	s
Time step size	Δt	s
Time step quantity	npt	–

In the potential single phase flow (only one incompressible fluid inside the reservoir), the height of oil zone undisturbed by the flow, H_o, is equal to the height of entire simulated portion of the reservoir.

The potential is known on the two sides (2) and (4), and on the free surface (3). Its value is constant and can be calculated through Eq. (3), where p is the total pressure given by:

$$p = p_o + p_t \tag{51}$$

where p_o is the pressure relative to the weight of oil column above the knot and p_t is the pressure at top of this oil column, i.e., the pressure that gas makes on the free surface. Substituting Eq. (51) into Eq. (3) and setting the pressures as relative heights, it has:

$$\Phi = \frac{p_t}{\rho g} + H_o \tag{52}$$

At the interface between oil and gas - free surface (3), the existing pressure is only that which the gas exerts on the oil (p_t). The pressure on free surface can be assumed to be zero, without loss of generality. Therefore, the entire domain has a constant potential and value equal to its height (H_o). All knots of the lateral boundaries (2) and (4), and of the free surface (3) have known potential given by:

$$\Phi_2 = \Phi_3 = \Phi_4 = H_o \tag{53}$$

where H_o is the height of oil zone measured by the z-coordinate of free surface undisturbed by the flow.

The lower limit (1) is the waterproof base of the reservoir. Consequently, there is no flow of oil in the normal to edge direction. The existing boundary condition is:

$$q_1 = 0 \tag{54}$$

The same simulator and boundary conditions are also applied in an axisymmetric quick drawdown problem where there is not a sink.

3.2.2 Potential Double Phase Flow

In this case, the domain of problem is defined as being homogeneous by parts, i.e., the numerical procedures, presented in each of the sub-regions are applied, as if they were separated from each other (Liggett and Liu [5]).

The homogeneity condition by sub-regions often occurs in engineering problems. Heat conduction in a solid composed of two distinct materials is an example where each material has a different thermal conductivity. Katsikadelis [29] cites the application of sub-region formulation in modeling composite bodies, where each component of the composite material is treated as a sub-region. For the case of double phase flow in porous media, addressed in this paper, it is also treated as being homogeneous by parts, since each sub-region (media) has different and homogeneous hydraulic conductivity K in all its extension according to the fluid that is saturating (according to the adopted model). Figure 3 shows the general appearance for a water coning problem.

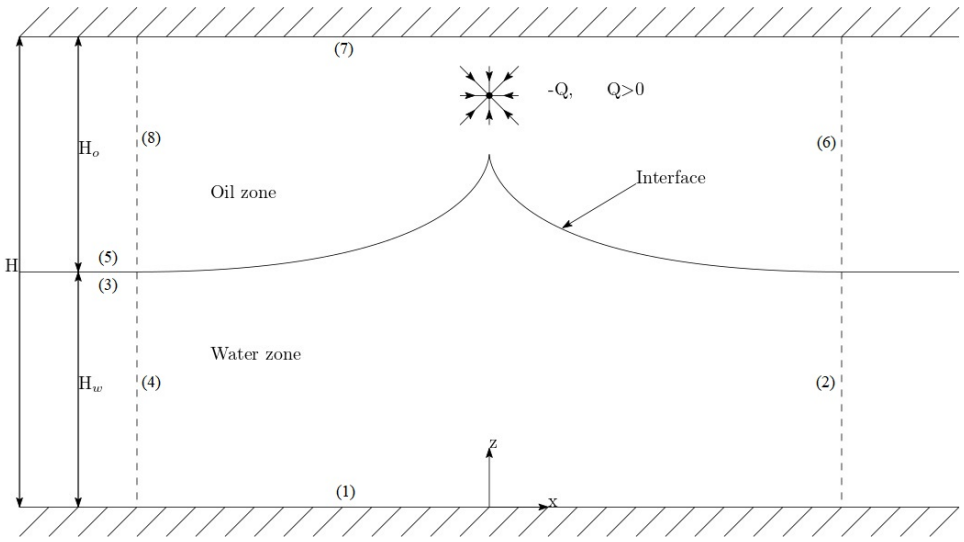

Fig. 3: Water Coning Phenomenon - Boundary Conditions: (1) and (7) impermeable boundary ($q = 0$); (2), (4), (6) and (8) known potential boundary; (3) and (5) interface boundary

The two sub-regions must share the same coordinate system as they form a single domain. However, each sub-region must be treated independently of each other. They are separated by an abrupt interface.

Upper Sub-region

The potential is known on both sides (6) and (8). Its value is constant and has a value equal to the total height of the simulated portion of the reservoir ($H_o + H_w$). Therefore, the potential for upper sub-region in which oil is contained in the reservoir can be calculated as:

$$\Phi_6 = \Phi_8 = H_o + H_w \tag{55}$$

The top pressure corresponding to the upper fluid column is assumed to be zero, without loss of generality.

Lower Sub-region

The potential is known on both sides (2) and (4). Its value is constant and related to the height values of each reservoir sub-region (H_o and H_w) and to the specific mass ratio between the lower and upper fluid ($\alpha = \rho_{R_1}/\rho_{R_2}$).

The reservoir top pressure can be assumed zero without loss of generality. Lateral boundaries (2) and (4) have known potential given by:

$$\Phi_2 = \Phi_4 = H_w + \frac{1}{\alpha} H_o \tag{56}$$

Impermeable Edges

The lower (1) and upper (7) edges are impermeable, i.e., there is no flow in the normal direction. Therefore, the existing boundary condition is identical to the potential single phase flow.

Interface Analysis

The major difference in determining boundary conditions between the potential single and double phase simulators is in the interface. According to Bear [4], the model used considers the fluids to be immiscible and the

approach to interface as being abrupt. The abrupt interface condition implies that for a point located on the interface, the velocity must have the same magnitude but opposite directions from the point of view of either fluid. The boundary conditions for the interface are the equations of pressure compatibility and velocity equilibrium, given through the flow phenomenon that leads to the pressure continuity condition between the two fluids, throughout the reservoir and, consequently, at the interface. Continuity means that pressure between two fluids is the same. Hair strains are considered to be negligible.

The pressure continuity equation must be written in terms of Φ, since the integral equation is written in terms of the potential Φ. Putting the pressure into evidence in Eq. (3), we have:

$$p = (\Phi - z)\,\rho g \tag{57}$$

The pressure continuity equation between the two fluids corresponding to the sub-region R_1 (lower sub-region) and R_2 (upper sub-region) at the interface is written as:

$$(\Phi_{R_1} - z_{R_1})\,\rho_{R_1} g = (\Phi_{R_2} - z_{R_2})\,\rho_{R_2} g \tag{58}$$

From the ratio of specific masses (α) and knowing that for a point on the interface, $z_{R_1} = z_{R_2} = z$, we have:

$$\Phi_{R_2} - \alpha\Phi_{R_1} = (1-\alpha)\,z \tag{59}$$

or

$$\Phi_5 - \alpha\Phi_3 = (1-\alpha)\,z \tag{60}$$

that is the potential compatibility equation for interface edge (3) and (5).

The potential is continuous within each sub-region, but has interface discontinuity; unlike pressure that is continuous throughout the domain. That is, the pressure is unique at each point of the interface, no matter which sub-region is contained. The normal flow to the interface has the same magnitude for both sub-regions, but opposite directions.

The velocity equilibrium equation at the interface is given by

$$q_5 + q_3 = 0 \tag{61}$$

Equation (61) is applied to interface collocation points, starting at the velocity after second collocation point and ending before last collocation point. Intermediate interface collocation points require extra equations in addition to these "coupling" equations. The extra equations are the same to those of the free surface of single phase simulators, given by Eq. (50) for each collocation point.

3.3 Solution method

At time $t = 0$, it is assumed that the interface is horizontal. The developed simulator solves the potential problem arising from the initial scenario by calculating the potentials and velocities in the normal direction throughout the boundary and at the interface collocation points. The next step is to calculate the new interface position through the calculated velocity by applying it to Eq. (50). As a result, the coordinates of each interface collocation point are obtained at the end of time step Δt.

A new scenario is then established for the next iteration. The boundary conditions are the same as those initially prescribed. The new interface position is no longer assumed as horizontal, but determined by the calculated coordinates. The code solves potential problem arising from this new scenario and performs the calculation of new interface position. This whole procedure is repeated until the flow at interface reaches a value near to zero. Thus, the evolution of interface over time is obtained.

4 Results

In this work, the results are presented for single phase potential simulator (only one incompressible fluid inside the reservoir), that is, to simulate the phenomenon of gas coning in order to be compared and validated for the Hele-Shaw cell. The results are also presented for double phase simulator (two incompressible fluids inside the reservoir) to simulate the phenomenon of water coning and to add more complexity for the new methodology validation. These results are applied in horizontal wells.

The axysimmetric geometries are also presented, demonstrating and validating the effectiveness of new tool developed in this work to study gas coning phenomena in axisymmetric oil reservoirs from vertical wells and quick drawdown problem in an aquifer (water reservoir); the Isogeometric Boundary Element Method for axisymmetric problems.

4.1 Hele-Shaw cell

The Hele-Shaw cell simulator was developed for comparison and validation with the potential single phase simulator (only one incompressible fluid inside the reservoir) that are inserted in Fortaleza et al. [2], in order to replicate the analytically solved case.

The settings for the Hele-Shaw cell are: 2.0 m wide, 4.0×10^{-1} m high liquid column and 4.0×10^{-3} m thick. The extracted fluid is glycerin, with specific mass $\rho = 1.255 \times 10^3$ kg/m^3 and dynamic viscosity $\mu = 1.0255$ Pa.s.

The simulator data are:

- Fluid potential $\Phi = 4.0 \times 10^{-1}$ m
- Well intensity (sink) $Q = -2.718 \times 10^{-3}$ m^2/s.
- Well coordinates (sink) $(x_p; z_p) = (1.0; 0.0)$ m.
- Total time analysis $t_t = 10^4$ s.
- Pump time on $t_p = 10^4$ s.
- Time step size $\Delta t = 1.0$ s.
- Time step amount $npt = 10^4$.

The hydraulic conductivity of the porous media is given by Zhang et al. [30], as a function of Hele-Shaw cell thickness, through the following expression:

$$K = \frac{\rho g b^2}{12\mu} \tag{62}$$

where b is the thickness of the Hele-Shaw cell and g is the gravity acceleration. Therefore, the calculated hydraulic conductivity $K = 1.601 \times 10^{-2}$ m/s.

Figure 4 presents the result for potential gradient with stable interface position at critical flow, in the simulated case (Hele-Shaw cell). That is, a single phase isogeometric potential simulator (only one incompressible fluid inside the reservoir) for the study of gas coning phenomenon in reservoirs with horizontal wells.

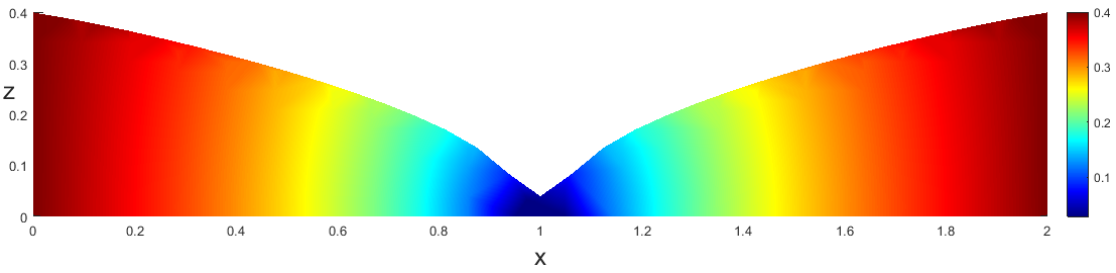

Fig. 4: Potential gradient with mobile interface at time $t = t_b = 10^4$ s (IGA-BEM). Hele-Shaw Cell

The stable interface position at critical flow for the single phase isogeometric potential simulator is shown in Fig. 5 with the others results from the Fortaleza et al. [2] work.

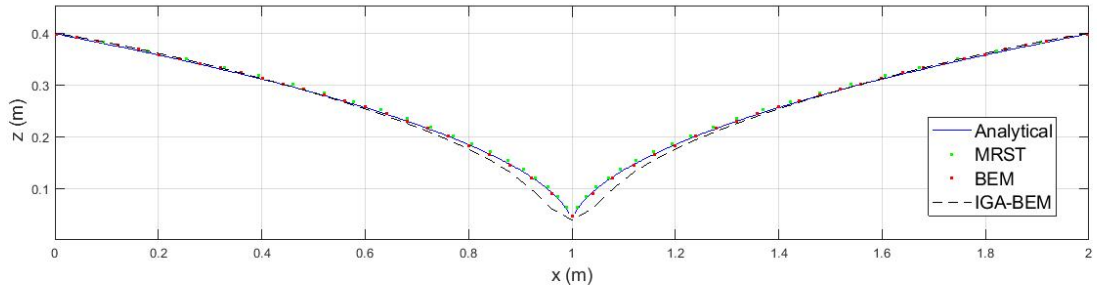

Fig. 5: Stable interface position at critical flow: Hele-Shaw cell. Comparing different results

Figure 5 shows the results for analytical, MATLAB Reservoir Simulation Toolbox (MRST), Boundary Element Method (BEM) and Isogeometric Boundary Element Method (IGA-BEM). The new tool to study gas coning - the single phase isogeometric potential simulator where only one incompressible fluid is inside the reservoir - presented good agreement with the other tools for the stable interface position at critical flow. The isogeometric formulation has a different behaviour close to the singularity due the imposing too high level of continuity close to it.

Finally, the result for Hele-Shaw cell simulation can be compared with the other results in the literature (Fortaleza et al., [2]), as well as for the analytically solved case, as can be seen from Table 2:

Table 2: Hele-Shaw Cell Simulator

Simulator	**Critical flow** [m/s]	**Center knot height** [m]
Analytical result	2.54×10^{-3}	4.243×10^{-2}
Potential single phase	2.59×10^{-3}	4.228×10^{-2}
Potential double phase	2.60×10^{-3}	4.416×10^{-2}
Isogeometric potential single phase	2.54×10^{-3}	3.877×10^{-2}

The result for the critical flow rate found by the simulator developed in this work showed exactly the same value for the analytical result, thus validating the new proposed methodology: IGA-BEM for the study of the gas coning phenomenon in homogeneous reservoirs with horizontal wells, through the use of a Hele-Shaw cell. For the isogeometric potential single phase case, there is an agreement up to the third digit regarding the analytical result. For the central knot height, however, it is showed an error of 8.6%. This difference can

be explained by the fact that both the analytical formulation and the formulation of the standard boundary elements (potential single phase and potential double phase), provide for the formation of a "spit", with a sharp corner indicating discontinuity in the derivative. Since the isogeometric formulation guarantees the continuity of the first derivative, the "spit" is not formed and the surface of the midpoint presents smooth. Therefore, the difference in the value of central knot height. A proposal to improve the agreement with analytical results, is the enrichment of NURBS with functions that allow discontinuity of the derivatives. However, this enrichment was outside the scope of this work.

The simulation validates the efficiency for the using of NURBS functions through the Boundary Element Method, to analyse the gas/water coning phenomenon into a homogeneous reservoir as a new alternative tool to study critical flows in wells.

4.2 Axisymmetric problems

This section presents results for the simulation of gas coning phenomenon through a new tool that was developed to study the behavior of oil extraction in an axisymmetric reservoir in a vertical well and, finally, for a quick drawdown problem in an aquifer.

4.2.1 Gas Coning - Vertical well

The settings for first geometry, gas coning phenomena, are: 1.0 m wide and 1.0 m oil column high. The extracted fluid is oil with specific mass $\rho_o = 1.245 \times 10^3$ kg/m^3 and dynamic viscosity $\mu_o = 4.0 \times 10^{-1}$ Pa.s.

The simulator data are:

- Hydraulic conductivity $K = 5.725 \times 10^{-3}$ m/s.
- Well intensity (sink) $Q = -5.697 \times 10^{-4}$ m^2/s.
- Well coordinates (sink) $(x_p; z_p) = (0.0; 5.0 \times 10^{-1})$ m.
- Total time analysis $t_t = 1.5 \times 10^3$ s.
- Pump time on $t_p = 1.5 \times 10^3$ s.
- Time step size $\Delta t = 5.0 \times 10^{-1}$ s.
- Time step amount $npt = 3.0 \times 10^3$.

Figure 6 shows the IGA-BEM code in an axisymmetric geometry - gas coning phenomena.

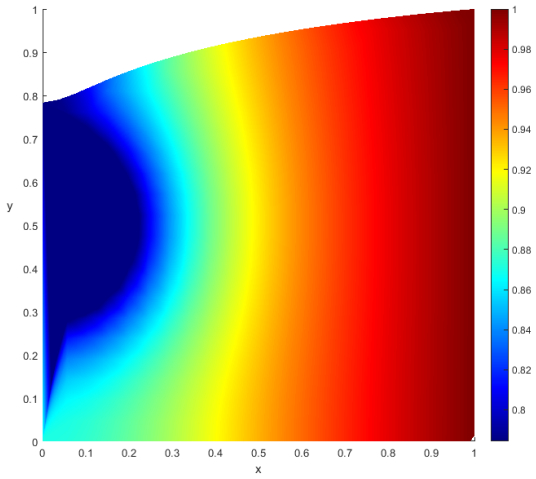

Fig. 6: Potential gradient in an axisymmetric reservoir (gas coning)

Figure 7 shows the comparison between both codes, Isogeometric Boundary Element Method and conventional Boundary Element Method, about variation of midpoint of the free surface in a reservoir with porosity $n = 0.2$. When the medium porosity is considered, the convergence velocity for the stabilization of the midpoint of the free surface is higher for both codes, since the real average velocity of the fluid inside pores increases according to Eq. (4). They basically present the same value to height of cone edge: 7.826×10^{-1} m and 7.832×10^{-1} m to AXI-BEM and AXI-IGA-BEM, respectively. A difference of 0.08 %.

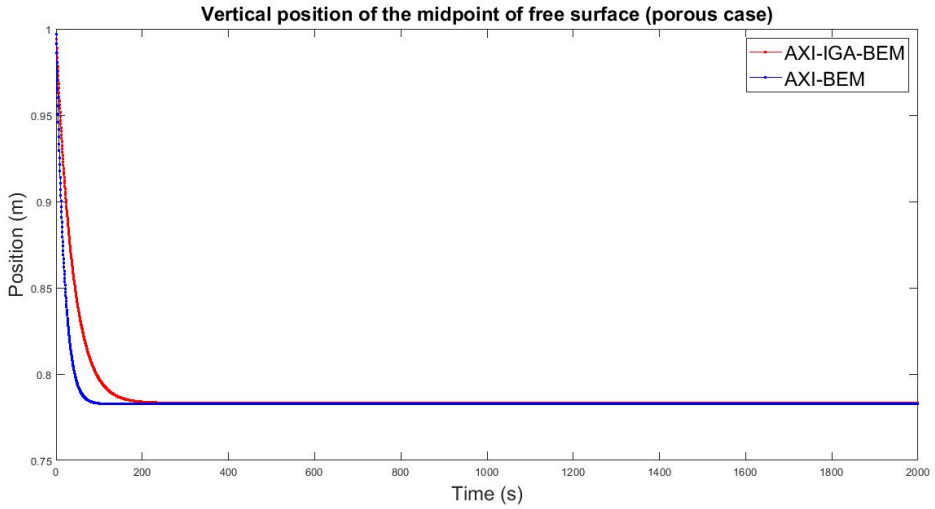

Fig. 7: Comparison between vertical position of the midpoint on free surface for AXI-IGA-BEM and AXI-BEM codes

The results showed that the code developed in this work (AXI-IGA-BEM) leads a higher time to stabilize than the AXI-BEM due the using of the NURBS functions. The reasons for the difference in the convergence

time between the AXI-IGA-BEM and the AXI-BEM have been studied, but no conclusions have been reached for this divergence. Since the formulation developed is quasi static, the time variable does not appear explicitly in this one. However, the real reasons are under study.

4.2.2 Quick Drawdown - Aquifer

A numerical experiment was carried out for the quick drawdown problem in an axisymmetric aquifer (water reservoir) for comparison with Rafiezadeh and Ashtiani [31] work using Boundary Element Method (BEM). They validated their work with the Hall [32] experiment tested in a 3D-axisymmetric sand tank and through of other researchers that solved it numerically. The present result is compared with Taylor and Luthin [33] work using Finite Difference Method (FDM) and with Cooley [34] work using Finite Element Method (FEM).

The axisymmetric problem can be compared directly with 3D problem since the three-dimensional object be developed through the rotation from a two-dimensional plane on an axial symmetry axis. If the loads are axisymmetric, you can analyze the ring using only a two-dimensional section representation as it is showed in this case for comparison.

For quick drawdown problems, the water level inside the axisymmetric well is dropped from H_e (external height) to a constant value H_w (well height) at $t = 0$ and stays at that level for all time. There is not a sink (or source) in quick drawdown problems.

The reservoir simulator data are:

- Hydraulic conductivity $K = 4.051 \times 10^{-3}$ m/s.
- Medium porosity $n = 0.3$.
- Well radius $r_w = 1.2192 \times 10^{-1}$ m.
- Well height $H_w = 3.048 \times 10^{-1}$ m.
- External radius $r_e = 1.9507$ m.
- External height $H_e = 1.2192$ m.
- Time step size $\Delta t = 6$ s.
- Time step amount $npt = 3.0 \times 10^2$.
- Total time analysis $t_t = 1.8 \times 10^3$ s.

The boundary conditions are shown in Fig. 8.

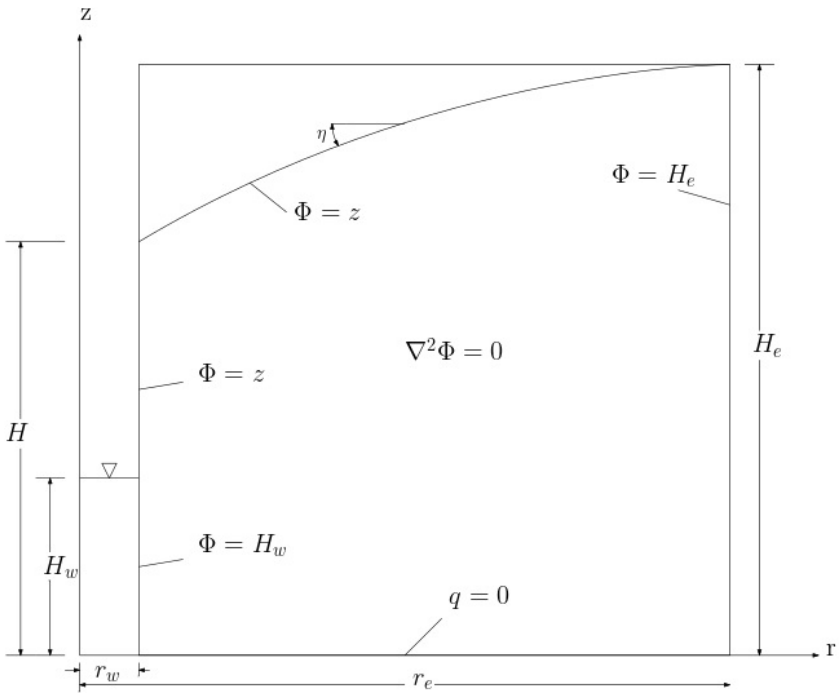

Fig. 8: Boundary conditions of the quick drawdown problem

1. $\Phi = H_e,\ r = r_e,\ 0 \leq z \leq H_e$.
2. $\Phi = H_w,\ r = r_w,\ 0 \leq z \leq H_w$.
3. $\Phi = z,\ r = r_w,\ H_w \leq z \leq H$.
4. $\lambda\,(t = 0) = \Phi = H_e,\ H_w\,(t = 0) = H\,(t = 0) = H_e$.
5. $q = 0,\ r_w \leq r \leq r_e,\ z = 0$.

The comparison of results are shown in the Fig. 9 through present axisymmetric modeling for the quick drawdown analysis in a Hall's well problem to isotropic case.

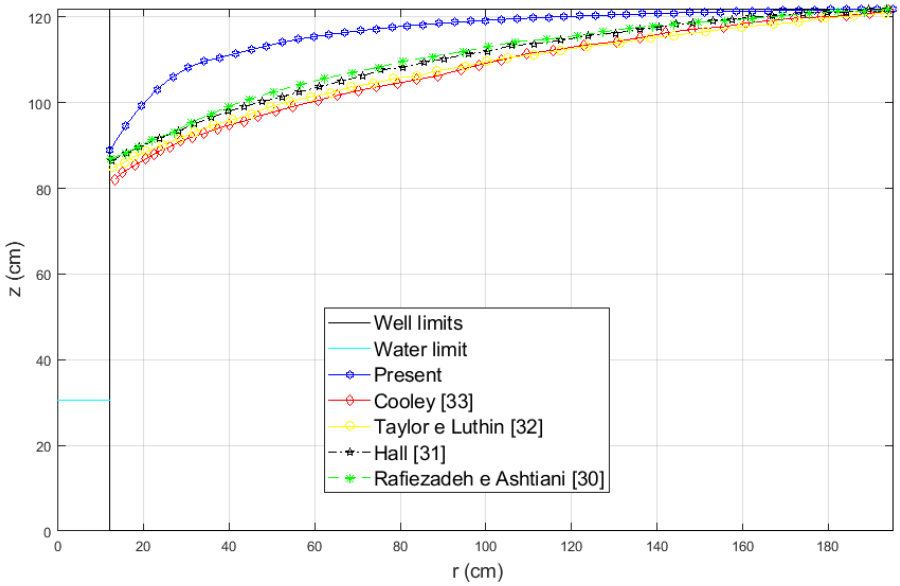

Fig. 9: Hall's well problem for isotropic case. Present result through axisymmetric modeling. Comparing different numerical methods for the quick drawdown analysis

The Hall's well problem in this case is applied only for a isotropic media. The final steady-state point for Rafiezadeh and Ashtiani [31] work is $H = 8.763 \times 10^{-1}$ m and for the present work is $H = 8.890 \times 10^{-1}$ m; a difference of 1.4 %. The result presents a good agreement with the others results in the literature adding a new contribution through axisymmetric modeling and Isogeometric Boundary Element Method (IGA-BEM) using NURBS curves.

4.3 Water coning

The potential double phase simulator was used to obtain an available result in an oil extraction reservoir scenario subject to the occurrence of water coning. The settings for the geometry are: 1.6 m wide, 2.0×10^{-1} m oil column high and 2.0×10^{-1} m water column high. The extracted fluid is oil with specific mass $\rho_o = 1.025 \times 10^3$ kg/m^3 and dynamic viscosity $\mu_o = 3.0 \times 10^{-4}$ Pa.s; the water has specific mass $\rho_w = 6.888 \times 10^2$ kg/m^3 and dynamic viscosity $\mu_w = 3.0 \times 10^{-3}$ Pa.s.

The simulator data are:

- Hydraulic conductivity (water sub-region) $K_w = 3.319 \times 10^{-5}$ m/s.
- Hydraulic conductivity (oil sub-region) $K_o = 2.23 \times 10^{-6}$ m/s.
- Well intensity (sink) $Q = -7.241 \times 10^{-7}$ m^2/s.
- Well coordinates (sink) $(x_p; z_p) = (8.0 \times 10^{-1}; 3.0 \times 10^{-1})$ m.
- Total time analysis $t_t = 3.0 \times 10^4$ s.
- Pump time on $t_p = 3.0 \times 10^4$ s.
- Time step size $\Delta t = 1.0$ s.
- Time step amount $npt = 3.0 \times 10^4$.

Figure 10 shows the evolution of deformed interface for the sub-critical flow found - last time step, 3.0×10^4 s.

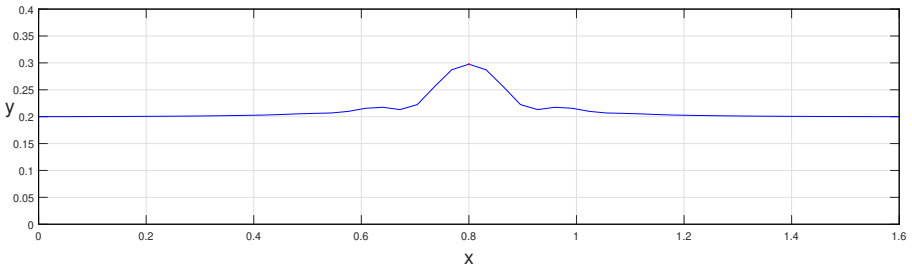

Fig. 10: Deformed interface for the sub-critical flow found - last time step

The result shows water coning phenomena growing into the reservoir as time passes and the tip of cone tends to touch the sink, as it is expected through literature (Ruiz et al., [35]). Therefore, this section adds one more contribution to validate the new methodology through the isogeometric formulation on the boundary elements method in a problem with more complexity.

5 Conclusions

The main characteristics and information regarding the simulator of horizontal and vertical wells (axisymmetric problem) in homogeneous reservoirs were gathered in this work. The discretization was carried out for the single and double phase potential flow model, in which it was developed through formulations of the Isogeometric Boundary Elements Method with application in axisymmetric problems for the study of phenomena of the gas/water coning in oil reservoirs, aquifers (water reservoirs) analysis as well as the existing boundary conditions.

The isogeometric formulation has two characteristics that differentiate them from the traditional formulation of the boundary element method, both arising from the fact that NURBS is used as shape functions instead of Lagrange polynomials. The first is that the geometries most commonly used in engineering problems, such as circumferences, ellipses, spheres, cylinders, among others, can be represented exactly. The second is that in NURBS there is continuity of derivatives up to the order $n-1$, that is not obtained by the use of Lagrange polynomials in the standard BEM.

An important contribution of this work was the development of an isogeometric formulation of the Boundary Element Method for axisymmetric problems, where no formulation of this type applied to IGA-BEM was found in the literature. The fundamental axisymmetric solution found in the literature in the implementations of the standard BEM, is obtained through the integration of the fundamental 3D solution around the axis of axial symmetry, which is used in the Isogeometric formulation presented in this work. The fundamental solutions are written according to elliptical integrals and the treatment of singularities in the influence matrices was carried out through the Telles Transform.

The union of NURBS type functions in the Integral Boundary Equation discretized together with fundamental axisymmetric solutions, has become a new tool used in simulation of axisymmetric problems. The results for the well simulator were compared with the literature and showed a good agreement between the

cases studied: Hele-Shaw cell (oil reservoir) and Hall well (water reservoir). The Axisymmetric formulation was validated by modeling problems in the literature that present analytical solutions.

The work showed that the IGA-BEM with application in axisymmetric problems is a new competitive tool not only for conventional BEM, but also for FDM, FVM and FEM. The method evidenced the efficacy in treatment of simplified multiphase flow problems in porous media, that is, homogeneous, incompressible and isotropic, where the dynamic viscosity of the fluids that saturate the rock are considered to be constant; especially when there are movable borders involved. The axisymmetric and isogeometric formulations allied to the BEM is an alternative to increase the precision of implemented algorithms. Besides, the amount of data necessary to model is reduced, providing a small linear system, with few degrees of freedom.

6 List of symbols

Roman

$\mathbf{A}$ = Unknown variables vector
A = Cross-sectional area
$\mathbf{b}$ = Unknown variables vector
B = Control points
b = Thickness
c = Multiplying constant
C = Curve function
$\mathbf{e}$ = Unit normal vector
$\mathbf{E}$ = Transformation matrix
F = Interface function
g = Gravity acceleration
$\mathbf{G}$ = Matrix
$\mathbf{H}$ = Matrix
H = Height
K = Hydraulic conductivity
L = Length
m = Parameter
$\mathbf{n}$ = Normal vector
n = Porosity
N = Basis function
p = Pressure; Load point
$\mathbf{q}$ = Apparent velocity vector
q = Volumetric flow rate per unit cross-sectional area
Q = Volumetric flow rate; Field point
r = Radial coordinate; Radius
R = Rational basis function
$\mathbf{s}$ = Sink vector
t = Time; Curve parameter
$\mathbf{u}$ = Real average velocity vector;
u = Knot vector values
$\mathbf{U}$ = Knots vector
$\mathbf{x}$ = Variable vector; Position vector
$\mathbf{V}$ = Translation vector
x = Ordinate axis
y = Abscissa axis
z = Vertical and axial coordinate

Greek

α = Specific mass ratio
β = Weighting factor
Γ = Boundary
δ = Dirac delta
Δ = Finite difference
∇ = Mathematical operator
η = Free surface slope angle
θ = Tangential direction
κ = Absolute permeability
λ = Interface height function
μ = Fluid dynamic viscosity
ρ = Fluid specific mass
Φ = Velocity potential (piezometric head)
ω = Weight function

Subscripts

axi = relative to the axial
d = relative to the source point
e = relative to the elliptic; relative to the external
g = relative to the gas
i = relative to the specific control point
j = relative to the quantity of sink
k = relative to the curve order
m = relative to the time step
o = relative to the oil
p = relative to the pump
s = relative to the sink
t = relative to the top; relative to the total
w = relative to the well; relative to the water
x = relative to the arbitrary control point
z = relative to the height of interface
$2D$ = relative to the two-dimensional
$3D$ = relative to the three-dimensional

Superscripts

c = relative to the control point

References

1. Dake LP (1983) Fundamentals of Reservoir Engineering, vol 8, 1st edn. Elsevier Science

2. Fortaleza ELF, Filho JOAL, Gontijo GSV, Albuquerque EL, Solimões RDP, Soares MM, Miranda MER, Abade GC (2019) Analytical, numerical and experimental study of gas coning on horizontal wells. Journal of the Brazilian Society of Mechanical Sciences and Engineering 12:1783–1810
3. Ramsak M, Skerget L (2014) A highly efficient multidomain bem for multimillion subdomains. Engineering Analysis with Boundary Elements 43:76–85
4. Bear J (1972) Dynamics of fluids in porous media. American Elsevier
5. Ligget JA, Liu PLF (1983) The boundary integral equation method for porous media flow. George Allen and Unwin
6. Lin F (1996) NURBS in CAD and Computer Graphics, 1st edn. Springer-Verlag
7. Piegl L, Tiller W (1996) The NURBS book. Springer-Verlag, Berlin, Germany
8. Rogers DF (2000) An introduction to NURBS: with historical perspective. Elsevier
9. Farin GE (1999) NURBS for Curve & Surface Design: From Projective Geometry to Practical Use. A K Peters/CRC Press
10. Piegl L (1991) On nurbs: a survey. IEEE Computer Graphics and Applications 11(1):55–71
11. Lamousin H, Waggenspack N (1994) Nurbs-based free-form deformations. IEEE Computer Graphics and Applications 14(6):59–65
12. Hughes T, Reali A, Sangalli G (2010) Efficient quadrature for nurbs-based isogeometric analysis. Computer Methods in Applied Mechanics and Engineering 199(5-8):301–313
13. Temizer I, Wriggers P, Hughes T (2011) Contact treatment in isogeometric analysis with nurbs. Computer Methods in Applied Mechanics and Engineering 200(9-12):1100–1112
14. Nielsen PN, Gersborg AR, Gravesen J, Pedersen NL (2011) Discretizations in isogeometric analysis of navier-stokes flow. Computer Methods in Applied Mechanics and Engineering 200(45):3242–3253
15. Bazilevs Y, Calo VM, Hughes TJR, Zhang Y (2008) Isogeometric fluid-structure interaction: theory, algorithms, and computations. Computational Mechanics 43(1):3–37
16. Bazilevs Y, Akkerman I (2010) Large eddy simulation of turbulent taylor-couette flow using isogeometric analysis and the residual-based variational multiscale method. Journal of Computational Physics 229(9):3402–3414
17. Hughes TJR, Cottrell JA, Bazilevs Y (2005) Isogeometric analysis: Cad, finite elements, nurbs, exact geometry and mesh refinement. Computer Methods in Applied Mechanics and Engineering 194:4135–4195
18. Cabral JJSP, Wrobel LC, Brebbia CA (1990) A bem formulation using b-splines: I-uniform blending functions. Engineering Analysis with Boundary Elements 7(3):136–144
19. Cabral, Wrobel LC, Brebbia CA (1991) A bem formulation using b-splines: Ii-multiple knots and non-uniform blending functions. Engineering Analysis with Boundary Elements 8:51–55
20. Simpson RN, Bordas SPA, Trevelyan J, Rabczuk T (2012) A two-dimensional isogeometric boundary element method for elastostatic analysis. Computer Methods in Applied Mechanics and Engineering 209:87–100
21. Simpson RN, Bordas SPA, Lian H, Trevelyan J (2013) An isogeometric boundary element method for elastostatic analysis: 2d implementation aspects. Computers and Structures 118:2–12
22. Wang D, Zhang H (2014) A consistently coupled isogeometric-meshfree method. Computer Methods in Applied Mechanics and Engineering 268:843–870
23. Shaw A, Roy D (2008) Nurbs-based parametric mesh-free methods. Computer Methods in Applied Mechanics and Engineering 197(17):1541–1567
24. Kim HJ, Youn SK (2012) Spline-based meshfree method. International Journal for Numerical Methods in Engineering 92(9):802–834
25. Campos LS, Albuquerque EL, Wrobel LC (2017) An aca accelerated isogeometric boundary element analysis of potential problems with non-uniform boundary conditions. Engineering Analysis with Boundary Elements 80:108–115
26. Lucas SK, Blake JR, Kucera" A (1991) A boundary-integral method applied to water coning in oil reservoirs. Journal of the Australian Mathematical Society 32:261–283

27. Bakr AA (1986) The boundary integral equation method in axisymmetric stress analysis problems. Springer-Verlag, Heidelberg, Germany
28. Becker AA (1992) The boundary element method in engineering: a complete course. McGraw-Hill
29. Katsikadelis JT (1984) The Boundary Element Method for Engineers and Scientists - Theory and Applications, 2nd edn. Springer-Verlag
30. Zhang H, Barray DA, Hocking GC (1999) Analysis of continuous and pulsed pumping of a phreatic aquifer. Advanced in Water Resources 22(6):623–632
31. Rafiezadeh K, Ataie-Ashtiani B (2014) Transient free-surface seepage in three-dimensional general anisotropic media by bem. Engineering Analysis with Boundary Elements 46:51–66
32. Hall H (1955) An investigation of steady flow toward a gravity well. La Houille Blanche 10:8–35
33. Taylor G, Luthin J (1969) Computer methods for transient analysis of water-table aquifers. Water Resources Research 5:144–152
34. Cooley R (1983) Some new procedures for numerical solution of variably saturated flow problems. Water Resources Research 19:1271–1285
35. Ruiz JAM, Chen B, Trevelyan J, Gourgiotis PA, Albuquerque EL (2019) Enriched bem for water coning. Proc UKBIM12 Conference, Oxford, UK pp 1–8